

# $^{75}\text{As}$ NMR studies of superconducting $\text{LaO}_{0.9}\text{F}_{0.1}\text{FeAs}$

H.-J. Grafe<sup>1</sup>, D. Paar<sup>1,2</sup>, G. Lang<sup>1</sup>, N. J. Curro<sup>3</sup>, G. Behr<sup>1</sup>, J. Werner<sup>1</sup>,  
J. Hamann-Borrero<sup>1</sup>, C. Hess<sup>1</sup>, N. Leps<sup>1</sup>, R. Klingeler<sup>1</sup>, B. Büchner<sup>1</sup>

<sup>1</sup>*IFW Dresden, Institute for Solid State Research, P.O. Box 270116, D-01171 Dresden, Germany*

<sup>2</sup>*Department of Physics, Faculty of Science, University of Zagreb, P. O. Box 331, HR-10002 Zagreb, Croatia*

<sup>3</sup>*Department of Physics, University of California, Davis, CA 95616, USA*

(Dated: October 25, 2018)

We have performed  $^{75}\text{As}$  Nuclear Magnetic Resonance (NMR) measurements on aligned powders of the new  $\text{LaO}_{0.9}\text{F}_{0.1}\text{FeAs}$  superconductor. In the normal state, we find a strong temperature dependence of the spin shift and Korringa behavior of the spin lattice relaxation rate. In the superconducting state, we find evidence for line nodes in the superconducting gap and spin-singlet pairing. Our measurements reveal a strong anisotropy of the spin lattice relaxation rate, which suggest that superconducting vortices contribute to the relaxation rate when the field is parallel to the  $c$ -axis but not for the perpendicular direction.

PACS numbers: 74.70.-b, 76.60.-k

The discovery of superconductivity in the iron-oxypnictide compounds has been focus of tremendous interest in recent months [1, 2]. These compounds have transition temperatures up to 55 K, yet the conventional BCS picture of a phonon-mediated pairing mechanism appears to be untenable due to the weak electron-phonon coupling [3, 4]. Rather, an unconventional pairing mechanism may be at work in these materials as in the high temperature superconducting cuprates [5, 6]. These compounds are particularly interesting as they are the first example of unconventional superconductivity with a large transition temperature in a non-cuprate transition metal compound. Yet like the cuprates, there is mounting evidence that the normal state of these materials can only be described by excitations of strongly correlated electronic states [7]. Furthermore, the superconductivity in these compounds emerges in close proximity to a magnetic ground state, which suggests that magnetic correlations may be relevant for superconductivity [8, 9, 10]. These observations highlight the need for detailed studies of the  $\text{LaO}_{1-x}\text{F}_x\text{FeAs}$  family in order to shed important light on the physics of both the cuprates and strongly correlated superconductors in general [11].

In order to investigate the nature of the superconductivity and the unusual normal state excitations, we have performed  $^{75}\text{As}$  Nuclear Magnetic Resonance (NMR) and Nuclear Quadrupolar Resonance (NQR) in  $\text{LaO}_{0.9}\text{F}_{0.1}\text{FeAs}$  for both random and oriented powder samples. In the superconducting state, our results reveal the presence of line nodes in the superconducting density of states. We find that the spin lattice relaxation rate,  $T_1^{-1}$ , varies as  $T^3$  for  $0.1T_c < T < T_c$  for  $\mathbf{H}_0 \perp c$ , which is characteristic of a d-wave superconductor. We also find that  $T_1^{-1}$  is anisotropic in the superconducting state, and is enhanced when  $\mathbf{H}_0$  has a component along the  $c$ -axis. This result probably reflects the two-dimensional nature of these materials, which consist of alternating layers of FeAs and  $\text{LaO}_{1-x}\text{F}_x$ . In a type-II superconductor,  $T_1^{-1}$

can be enhanced in applied fields due to the presence of superconducting vortices [12, 13]. Surprisingly we find no enhancement for  $\mathbf{H}_0 \perp c$ ; this result suggests that either the vortices do not exist for this orientation, or they are pinned between the FeAs planes. In the normal state, we find that both  $(T_1T)^{-1}$  and the spin shift,  $K_s$ , are strongly temperature dependent, and decrease with decreasing temperature. The temperature dependent Knight shift is similar to the pseudogap behavior observed in underdoped high temperature superconductors [14, 15, 16, 17]. However, in contrast to the cuprates,  $(T_1T)^{-1}$  shows no evidence for antiferromagnetic fluctuations of local 3d spins. In fact, we find that the Korringa relation is satisfied for the As between  $T_c$  and 300 K, indicating that the dominant relaxation mechanism is via spin-flip scattering with itinerant quasiparticles, rather than via transferred coupling to fluctuating Fe 3d moments.

Polycrystalline samples of  $\text{LaO}_{0.9}\text{F}_{0.1}\text{FeAs}$  were prepared by standard methods as described in [18]. The crystal structure and the composition were investigated by powder x-ray diffraction and wavelength-dispersive x-ray spectroscopy (WDX). The magnetic susceptibility was measured in external fields  $10 \text{ Oe} < H < 70 \text{ kOe}$  using a SQUID magnetometer, and resistance was measured with a standard 4-point geometry. A value of  $T_c \approx 26.0 \text{ K}$  was extracted from these measurements. [19] The material was then ground to a powder with grain size approximately 1-100  $\mu\text{m}$ , mixed with Stycast 1266 epoxy in a mass ratio of 24:70, and allowed to cure in an external field of 9.2 T. NMR spectra of the  $^{75}\text{As}$  ( $I = 3/2$ ,  $\gamma = 7.2917 \text{ MHz/T}$ , 100 % abundance) in the random powder were obtained by summing the Fourier transform of the spin-echo signal as a function of frequency in a fixed magnetic field of 7.0494 T [20]. Typical powder spectra are shown in Fig. 1.  $^{75}\text{As}$  has a large quadrupolar moment ( $Q = 0.3b$ ) that interacts with the local electric field gradient (EFG) in

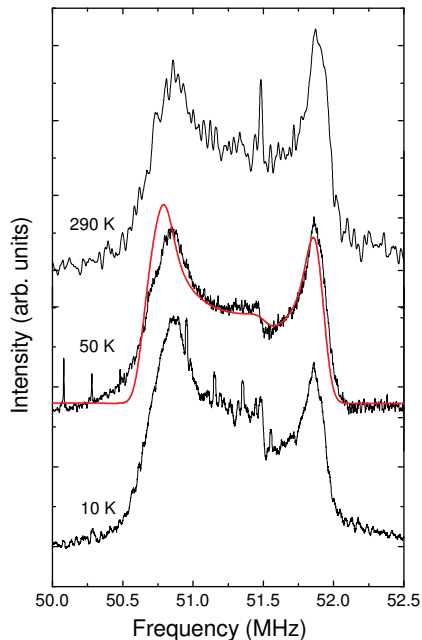


FIG. 1: (Color online) Frequency swept  $^{75}\text{As}$  NMR powder spectra of  $\text{LaO}_{0.9}\text{F}_{0.1}\text{FeAs}$  measured at  $H_0 = 7.0494$  T. The solid red line is a simulation of the powder spectrum as described in the text.

the crystal. The nuclear spin Hamiltonian is given by:  $\mathcal{H} = \gamma\hbar H_0(1 + K)\hat{I}_z + \frac{\hbar\nu_Q}{6}[(3\hat{I}_{z'}^2 - \hat{I}^2) + \eta(\hat{I}_{x'}^2 - \hat{I}_{y'}^2)]$ , where  $K$  is the magnetic shift,  $\nu_Q$  is the NQR frequency,  $V_{\alpha\beta}$  is the EFG tensor, and  $\eta$  is the asymmetry parameter of the EFG. Note that the principle axes  $\{x', y', z'\}$  of the EFG tensor are defined by the local symmetry in the unit cell, thus the resonance frequency of a particular nuclear transition,  $f(\theta, \phi)$ , is a strong function of field direction relative to the crystalline axes. For a powder, the external field is oriented randomly and the spectrum is typically quite broad. However, peaks in the powder pattern correspond to stationary points of the function  $f$ . Fig. 1 shows the powder pattern central transition ( $I_z = 1/2 \leftrightarrow -1/2$ ) of the As, and the two horn peaks correspond to crystallites with  $\theta \approx 41.8^\circ$  (lower frequency peak), and to  $\theta = 90^\circ$  (upper frequency peak), where  $\theta$  is the angle between  $z$  and  $z'$  [21]. The solid red line is a simulation of the powder pattern including both EFG and anisotropic spin shift effects. We find that the spectrum can be fit reasonably well with  $K_a = K_b = 0.14\%$ ,  $K_c = 0.2\%$ ,  $\nu_Q = 10.9$  MHz, and  $\eta = 0.1$ . We have also done zero-field NQR of the As, and found  $\nu_Q = 11.00(5)$  MHz.

Spectra for the oriented powder are shown in Fig. 2 for  $\mathbf{H}_0$  parallel to the orientation direction. Clearly, the

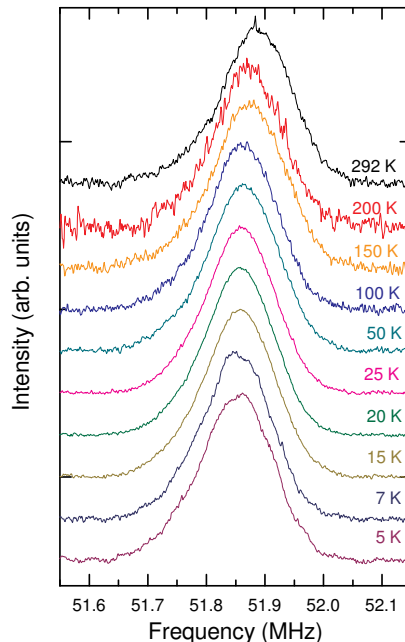


FIG. 2: (Color online)  $^{75}\text{As}$  NMR spectra of the oriented powder measured with  $\mathbf{H}_0 \perp c$  and  $H_0 = 7.0494$  T.

alignment process works well, as the linewidth of the oriented sample is nearly an order of magnitude smaller and the powder pattern structure has disappeared. The orientation of the powder was measured by x-ray diffraction and high field magnetization measurements. We find that the magnetic susceptibility is greatest in the plane ( $\mathbf{H}_0 \parallel ab$ ), where the crystal  $a$  and  $b$  axes are magnetically equivalent. The alignment axis of the powder is thus parallel to the  $ab$  direction, which is consistent with our observation that the resonance frequency of the aligned powder corresponds with the upper horn of the powder pattern. Therefore, the principle axis of the EFG with the largest eigenvalue must lie along the crystal  $c$ -axis. The As has four nearest neighbor Fe atoms, and lies just above or below the Fe plane. This site is axially symmetric, which is consistent with our observation that  $\eta \approx 0$ .

The resonance frequency,  $f$ , of the spectra in Fig.2 is given by:  $f = \gamma H_0(1 + K_{ab}) + 3\nu_Q^2/16\gamma H_0$  for  $\eta = 0$ . We have measured that  $\nu_Q$  is independent of temperature, therefore the temperature dependence is entirely due to the magnetic shift,  $K_{ab}$ . Fig. 3 shows  $K_{ab}(T)$  as a function of temperature, measured along the orientation axis of the sample. The magnetic shift arises from the interactions between the As nuclei and the surrounding electrons; generally it can be divided into  $K_{\text{tot}} = K_s + K_{\text{orb}}$ , where  $K_s = A\chi_{\text{spin}}$  arises via a hyperfine coupling to electron spins, and  $K_{\text{orb}}$  arising from orbital magnetiza-

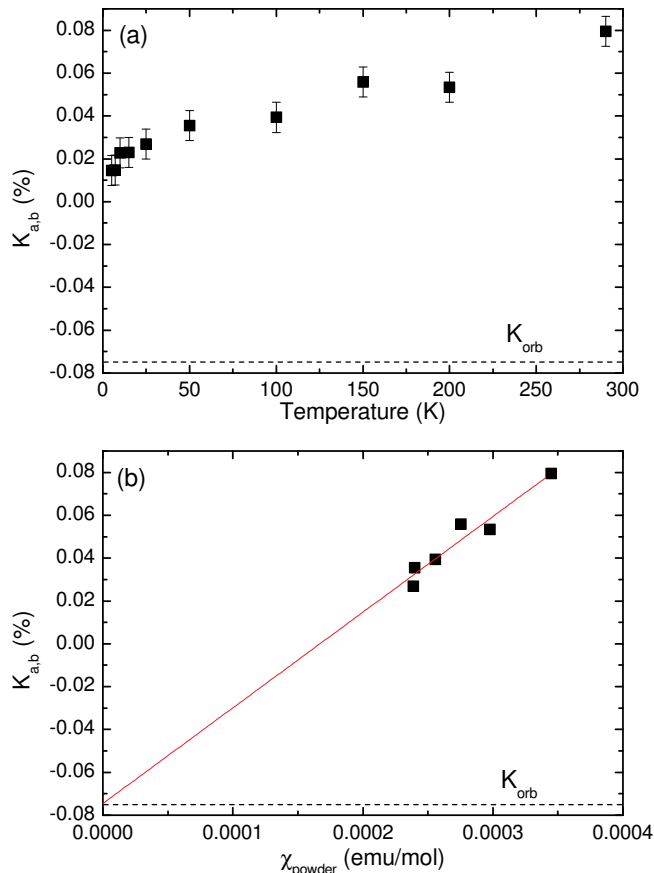


FIG. 3: (Color online) (a) Magnetic shift,  $K_{ab}$  versus temperature in the aligned sample. The dashed line indicates  $K_{orb}$  (b):  $K_{ab}$  versus  $\chi_{powder}$ , the magnetic susceptibility of the powder sample. The solid line is a fit as described in the text.

tion induced at the nuclear site [21]. In order to measure the hyperfine coupling, we have also measured the bulk magnetic susceptibility of the powder sample. Fig. 3b shows  $K_{ab}$  versus  $\chi_{powder}$  with temperature as an implicit parameter [22]. A linear fit to this data yields a hyperfine coupling  $A = 25(3)$  kOe/ $\mu_B$  plus an offset of  $K_{orb} = -0.075$  %. Note that this is assuming negligible diamagnetic and Van Vleck contributions to  $\chi_{powder}$ . If these contributions are to represent 50 % of  $\chi_{powder}$ ,  $K_{orb}$  is reduced to  $-0.008$  % [23]. The striking feature in Fig. 3a is a suppression of spin susceptibility with decreasing temperature in the normal state. This behavior is identical to that of the pseudogap in the cuprates, and has been observed in  $^{19}\text{F}$  NMR for  $x = 0.11$  [14, 16]. In the superconducting state, we find that  $K_{ab}$  decreases as well, which is suggestive of spin-singlet pairing.

We have measured the spin-lattice relaxation rate,  $T_1^{-1}$ , in both the normal and superconducting states. The relaxation was measured by inversion recovery of the longitudinal magnetization, and the data are well fit to

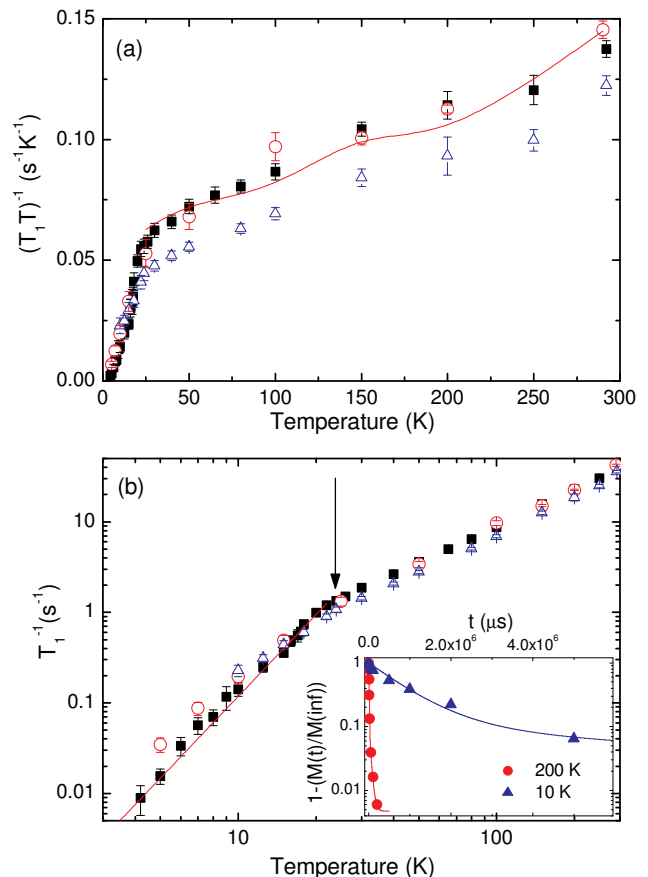


FIG. 4: (Color online) (a) The  $^{75}\text{As}$   $(T_1T)^{-1}$  versus temperature in  $\text{LaO}_{0.9}\text{F}_{0.1}\text{FeAs}$  measured at the upper horn ( $\blacksquare$ ,  $\theta = 90^\circ$ ), the lower horn ( $\triangle$  (blue),  $\theta \approx 41.8^\circ$ ), and in the aligned sample ( $\circ$  (red),  $\theta = 90^\circ$ ). The solid line is given by  $K_s^2(T)/\alpha\kappa$  as described in the text. (b)  $T_1^{-1}$  versus temperature. The arrow indicates  $T_c = 23.5$  K at 7T, and the solid line indicates  $T_1^{-1} \sim T^3$ , indicative of line nodes. Inset: Magnetization recovery and fits for two temperatures.

the standard expression for the central transition of a spin  $I = 3/2$  nucleus with a single  $T_1$  component (see inset of Fig.4). We measured  $T_1^{-1}$  on both peaks of the powder sample and on the aligned sample; the data are compared in Fig. 4a. The center frequency of the aligned powder spectrum and the upper horn of the powder pattern agree well, supporting our conclusion that the main axis of the EFG is perpendicular to the alignment axis ( $ab$ ). The  $(T_1T)^{-1}$  data for  $\theta \approx 41.8^\circ$  agrees reasonably with the data from Nakai *et al.* [17] below  $T \approx 200$  K. However, Nakai *et al.* have measured  $(T_1T)^{-1}$  at the center of the powder spectrum close to the unshifted frequency. The temperature dependence of  $T_1^{-1}$  is well described by a Korringa relation within experimental uncertainty. The solid line in Fig. 4a is a plot of  $K_s^2(T)/\alpha\kappa$ , where  $\kappa$  is the Korringa constant:  $\kappa = \hbar\gamma_e^2/4\pi k_B^{75}\gamma^2$ ,  $\gamma_e$  is the gy-

romagnetic ratio of the electron,  $k_B$  is the Boltzmann constant, and  $\alpha = 1.8$  is a constant. A linear scaling ( $(T_1T)^{-1} \sim K_s$ ) was suggested for  $x = 0.11$  via  $^{19}\text{F}$  NMR [16]. This behavior is surprising, since this material is close to an SDW quantum critical point and fluctuations of Fe 3d moments are a possible source for spin lattice relaxation [25]. It is not clear if the hyperfine coupling  $A$  represents an on-site contact interaction, or a transferred interaction to nearest neighbor Fe. If the coupling is transferred, then the symmetric location of the As can render it insensitive to magnetic fluctuations at the anti-ferromagnetic wavevector; such is the case for the oxygen site in  $\text{YBa}_2\text{Cu}_3\text{O}_{6+y}$  which also shows Korringa behavior even though the Cu 3d spins are strongly correlated [15]. However, in the  $\text{LaO}_{1-x}\text{F}_x\text{FeAs}$ , Nakai *et al.* have observed a dramatic enhancement of the As  $T_1^{-1}$  at lower doping levels when the system undergoes a spin density wave transition [17]. Therefore, the As form factor must not entirely cancel at the ordering wavevector. In contrast with the cuprates, we find no evidence of a pseudo-gap peak in  $(T_1T)^{-1}$  at a temperature  $T^* > T_c$  up to 300 K, nor any scaling of  $(T_1T)^{-1}$  with  $T/T_c$  in the normal state [26, 27]. The pseudogap peak was used to define the energy scale  $T^*$  of the pseudogap in underdoped cuprates. It is the temperature where  $(T_1T)^{-1}$  of the Cu shows a broad maximum. Our result suggests that either the As is insensitive to antiferromagnetic fluctuations, or these fluctuations have disappeared by  $x = 0.10$ .

In the superconducting state, we find that  $T_1^{-1}$  exhibits a drop at  $T_c$ , with no evidence for a Hebel-Slichter coherence peak. For  $T \ll T_c$ ,  $T_1^{-1}$  varies as  $T^3$ , as seen in Fig. 4. This behavior is indicative of line nodes in the superconducting gap function,  $\Delta(\mathbf{k})$ , and contrasts with the exponential behavior ( $T_1^{-1} \sim \exp(-\Delta/k_B T)$ ) expected for an isotropic superconducting gap. In the presence of an external magnetic field, we find that  $T_1^{-1}$  is anisotropic below  $T_c$ . As seen in Fig. 4b,  $T_1^{-1}$  is greater for  $\theta \approx 41.8^\circ$  than for  $\theta = 90^\circ$ . This result suggests that in addition to the excited quasiparticles, superconducting vortices may contribute to  $T_1^{-1}$ . In particular, the vortices can give rise to Doppler shifted quasiparticles in extended states outside the vortex cores, or may be contributing a dynamical field from simple vortex motion [28]. The net effect is an increase in  $T_1^{-1}$  above the  $T^3$  behavior expected in zero field. Surprisingly, for  $\mathbf{H}_0 \perp c$  we find no such enhancement down to 4 K. This absence suggests that the vortices may be pinned between FeAs layers, and therefore do not contribute to the relaxation rate at the As site. Similar effects have been observed in other layered superconductors [13], and may be a natural result of the short superconducting coherence length,  $\xi_c$ , along the  $c$ -direction.

In summary, we have measured the As NMR and NQR in the normal and superconducting states of  $\text{LaO}_{0.9}\text{F}_{0.1}\text{FeAs}$  and find evidence for line nodes in the superconducting gap function, and a pseudo-spin gap in

the normal state. This pseudo-spin gap gives rise to a suppression of  $K_s$  and  $T_1^{-1}$  for temperatures below 300 K.

We thank S.-L. Drechsler, W. Pickett and R. Singh for helpful discussions, and M. Deutschmann, S. Müller-Litvanyi, R. Müller, R. Vogel and A. Köhler for experimental support. This work has been supported by the DFG, through FOR 538. G. L. acknowledges support from the Alexander von Humboldt-Stiftung.

- 
- [1] Y. Kamihara, T. Watanabe, M. Hirano, and H. Hosono, *J. Am. Chem. Soc.* **130**, 3296 (2008).
  - [2] H. Takahashi, K. Igawa, K. Arii, Y. Kamihara, M. Hirano, and H. Hosono, *Nature* **453**, 376 (2008).
  - [3] L. Boeri, O. V. Dolgov, and A. A. Golubov (2008), arXiv:0803.2703.
  - [4] S.-L. Drechsler, M. Grobosch, K. Koepf, G. Behr, A. Köhler, J. Werner, A. Kondrat, N. Leps, R. Klingeler, C. Hess, R. Schuster, B. Büchner, M. Knupfer, (2008), arXiv:0805.1321.
  - [5] C. de la Cruz, Q. Huang, J. W. Lynn, J. Li, W. Ratcliff, J. L. Zarestky, H. A. Mook, G. F. Chen, J. L. Luo, N. L. Wang, et al. (2008), arXiv:0804.0795.
  - [6] P. Monthoux, D. Pines, and G. G. Lonzarich, *Nature* **450**, 1177 (2007).
  - [7] K. Haule and G. Kotliar (2008), arXiv:0805.0722.
  - [8] Z. P. Yin, S. Lebegue, M. J. Han, B. Neal, S. Y. Savrasov, and W. E. Pickett (2008), arXiv:0804.3355.
  - [9] J. Dong, H. J. Zhang, G. Xu, Z. Li, G. Li, W. Z. Hu, D. Wu, G. F. Chen, X. Dai, J. L. Luo, et al. (2008), arXiv:0803.3426.
  - [10] H.-H. Klauss, H. Luetkens, R. Klingeler, C. Hess, F. J. Litterst, M. Kraken, M. M. Korshunov, I. Eremin, S.-L. Drechsler, R. Khasanov, A. Amato, et al. (2008), arXiv:0805.0264.
  - [11] N. J. Curro, T. Caldwell, E. D. Bauer, L. A. Morales, M. J. Graf, Y. Bang, A. V. Balatsky, J. D. Thompson, and J. L. Sarrao, *Nature* **434**, 622 (2005).
  - [12] N. J. Curro, T. Imai, C. P. Slichter, and B. Dabrowski, *Phys. Rev. B* **56**, 877 (1997).
  - [13] S. M. De Soto, C. P. Slichter, H. H. Wang, U. Geiser, and J. M. Williams, *Phys. Rev. Lett.* **70**, 2956 (1993).
  - [14] H. Alloul, T. Ohno, and P. Mendels, *Phys. Rev. Lett.* **63**, 1700 (1989).
  - [15] P. C. Hammel, M. Takigawa, R. H. Heffner, Z. Fisk, and K. C. Ott, *Phys. Rev. Lett.* **63**, 1992 (1989).
  - [16] K. Ahilan, F. L. Ning, T. Imai, A. S. Sefat, R. Jin, M. A. McGuire, B. C. Sales, and D. Mandrus (2008), arXiv:0804.4026.
  - [17] Y. Nakai, K. Ishida, Y. Kamihara, M. Hirano, and H. Hosono (2008), arXiv:0804.4765.
  - [18] X. Zhu, H. Yang, L. Fang, G. Mu, and H.-H. Wen (2008), arXiv:0803.1288.
  - [19] H. Luetkens, H.-H. Klauss, R. Khasanov, A. Amato, R. Klingeler, I. Hellmann, N. Leps, A. Kondrat, C. Hess, A. Köhler, et al. (2008), arXiv:0804.3115.
  - [20] W. G. Clark, M. E. Hanson, F. Lefloch, and P. Ségransan, *Rev. Sci. Instr.* **66**, 2453 (1995).
  - [21] C. P. Slichter, *Principles of Nuclear Magnetic Resonance*

- (Springer-Verlag, 1992), 3rd ed.
- [22] The oriented sample contained a small paramagnetic impurity phase with an increasing susceptibility with decreasing temperature; therefore we plot  $K_{ab}$  versus  $\chi_{\text{powder}}$ , which contains no paramagnetic impurity phase.
- [23] Plotting  $(T_1T)^{-1/2}$  versus  $K_{ab}$ , and extrapolating to  $(T_1T)^{-1/2} = 0$  [24], gives similar results of  $K_{\text{orb}}$ .
- [24] M. Bankay, M. Mali, J. Roos, and D. Brinkmann, Phys. Rev. B **50**, 6416 (1994).
- [25] Q. Si and E. Abrahams (2008), arXiv:0804.2480.
- [26] V. Barzykin and D. Pines, Phys. Rev. B **52**, 13585 (1995).
- [27] N. Curro, Z. Fisk, and D. Pines, MRS Bulletin **30**, 442 (2005).
- [28] N. J. Curro, C. Milling, J. Haase, and C. P. Slichter, Phys. Rev. B **62**, 3473 (2000).